DIRECT PEPTIDE INTERACTION WITH SURFACE GLYCOSAMINOGLYCANS CONTRIBUTE TO THE CELL PENETRATION OF MAUROCALCINE

Narendra Ram[1], Sonia Aroui[1], Emilie Jaumain[1], Hicham Bichraoui[1], Rémy Sadoul[2], Kamel Mabrouk[3], Michel Ronjat[1], Hugues Lortat-Jacob[4] & Michel De Waard[1*]

INSERM U836, Grenoble Institute of Neurosciences, Research group 3, Calcium Channels, Functions and Pathologies laboratory, 38042 Grenoble Cedex 9, Université Joseph Fourier, France[1], INSERM U836, Grenoble Institute of Neurosciences, Research group 2, Neurodégénérescence et Plasticité, 38042 Grenoble Cedex 9, Université Joseph Fourier, France [2], Université Aix-Marseille 1, 2 & 3, CNRS-UMR 6517, Chimie, Biologie et Radicaux Libres, 15521 Avenue Esc. Normandie Niemen, 13397 Marseille Cedex 20, France[3], Institut de Biologie Structurale, UMR 5075 CEA/CNRS/Université Joseph Fourier, 41 rue Jules Horowitz, 38027 Grenoble Cedex 1, France[4].

Running head: Maurocalcine interacts with glycosaminoglycans.

Address correspondence to: Dr. Michel De Waard, Tel.: (33) 4 56 52 05 63,
E-mail: michel.dewaard@ujf-grenoble.fr

Maurocalcine (MCa), initially identified from a tunisian scorpion venom, defines a new member of the family of cell penetrating peptides (CPPs) by its ability to efficiently cross the plasma membrane. The initiating mechanistic step required for the cell translocation of a CPP implicates its binding onto cell surface components such as membrane lipids and/or heparan sulfate proteoglycans (HSPGs). Here, we characterized the interaction of wild-type MCa and MCa K20A, a mutant analogue with reduced cell-penetration efficiency, with heparin (HP) and heparan sulfates (HS) through surface plasma resonance (SPR). HP and HS bind both to MCa, indicating that HSPGs may represent an important entry route of the peptide. This is confirmed by the fact that (i) both compounds bind with reduced affinity to MCa K20A, and (ii) the cell penetration of wild-type or mutant MCa, coupled to fluorescent streptavidin, is reduced by about 50% in mutant CHO cell lines lacking either all glycosaminoglycans (GAGs) or just HS. Incubating MCa with soluble HS, HP or chondroitin sulfates (CS), also inhibits the cell penetration of MCa/streptavidin complexes. Analyses of the cell distributions of MCa/streptavidin in several CHO cell lines show that the distribution of the complex coincides with the endosomal marker lysotracker red and is not affected by the absence of GAGs. The distribution of MCa/streptavidin is not coincident with that of transferin receptors, nor affected by a dominant-negative dynamin 2 K44A mutant, an inhibitor of clathrin-mediated endocytosis. However, entry of the complex is greatly diminished by amiloride, indicating the importance of macropinocytosis in MCa/streptavidin entry. It is concluded that: i) interaction of MCa with GAGs quantitatively improves the cell penetration of MCa, and ii) GAG-dependent and –independent MCa penetration rely similarly on the macropinocytosis pathway.

Maurocalcine (MCa) is a 33-mer peptide isolated from the venom of the scorpion *Scorpio maurus palmatus.* MCa is a highly basic peptide since 12 out of 33 residues are positively charged including the amino terminal Gly residue, seven Lys residues and four Arg residues. Because it contains only four negatively charged residues, the net global charge of the peptide is also positive. MCa possesses three disulfide bridges connected according to the pattern Cys_3–Cys_{17}, Cys_{10}–Cys_{21}, and Cys_{16}–Cys_{32}. ^{1}H-NMR analysis further indicates that MCa folds along an inhibitor cystine knot motif (1). MCa contains three β-strands running from amino acid residues 9–11 (strand 1), 20–23 (strand 2), and 30–33 (strand 3), respectively, with β-strands 2 and 3 forming an antiparallel β-sheet. MCa has proven to be a highly potent modulator of the skeletal muscle ryanodine receptor type 1 (RyR1), an intracellular calcium channel. Addition of MCa to the extracellular medium of cultured myotubes induces Ca^{2+} release from the sarcoplasmic reticulum (SR) into the cytoplasm within seconds, as shown using a calcium-imaging approach (2,3). These observations, suggested that MCa is able to cross the plasma membrane to reach its pharmacological target. This was first demonstrated when a

biotinylated analogue of MCa was coupled to a fluorescent derivative of streptavidin and the complex shown to cross the plasma membrane (4). Cell penetration of this MCa-based complex is rapid, reaches saturation within minutes, and occurs at concentrations as low as 10 nM (5). Furthermore, an alanine scan of MCa indicates the importance of basic amino acid residues in the cell penetration mechanism. Reducing the net positive charge of the molecule appears to decrease its cell penetration efficiency. In parallel, MCa analogues exhibiting decreased penetration efficiency were also found to present reduced affinity for negatively charged lipids of the plasma membrane (6).

Over the past years, several peptides have been characterized for their ability to cross the plasma membrane (7-11). Cell penetration of peptides obeys three fundamental steps: (i) binding to some components of the plasma membrane, (ii) the cell entry process *per se*, and (iii) the subsequent release into the cytoplasm. Obviously, none of these steps are well understood and conflicting reports have emerged that may well arise from differences in the nature of the cell penetrating peptide (CPP) considered, cell preparations, experimental conditions, type of linkage to cargoes, or even cargo nature. Two non-competing mechanisms have been proposed for the cell entry of CPP. One is direct translocation through the plasma membrane by the CPP-induced reorganization of the membrane following several possible structural alterations (7-11). According to some investigators, this mechanism implies a direct CPP interaction with negatively charged lipids of the plasma membrane. This mechanism of penetration would be independent of both cell metabolic energy and membrane receptor presence. For instance, it was proposed that penetratin binds to the polar heads of lipids leading to the formation of inverted micelles, followed by a subsequent opening of these micelles inside the cell and the release of the peptide into the cytoplasm (12). A second mechanism involves a form of endocytosis by which the CPP gets localized into late endosomes from where it may eventually leak out partially towards the cytoplasm. Endocytosis can be initiated by binding of CPPs to HS along with binding to negatively charged moieties on the cell surface, such as lipids (13). Lipid-raft dependent macropinocytosis has been evidenced as one endocytosis pathway for the cell entry of CPPs (14,15). For instance, cellular uptake of a recombinant GST-TAT-GFP fusion protein depends on the presence of HS proteoglycans (HSPG) at the cell surface (16). Nevertheless, the role of GAGs in the cell penetration of CPPs remains debated. Stereochemistry, chain length, patterns of sulfation and negative charge distribution of GAGs lead to a great variety of protein binding motifs. Furthermore, the CPP structure also appears to determine its specificity for HSPG (17).

In the present study, we show that MCa interacts with GAGs such as HS and HP with apparent affinities in the micromolar range. A less penetrating analogue of MCa (MCa K20A) also shows a reduced apparent affinity for these GAGs suggesting a direct link between GAG interaction and cell penetration. Cell penetration of MCa_b-streptavidin complex is strongly inhibited by an inhibitor of macropinocytosis indicating that this route of entry is responsible for MCa penetration. However, use of GAG-deficient cell lines indicates that half of the cell penetration of the complex is conserved and still relies on macropinocytosis. We conclude that GAG-dependent and –independent entries of MCa use similar pathways. Cell surface GAGs appear important to specify a higher cell penetration level, but penetration still can occur in their absence presumably because binding onto lipids can also activate macropinocytosis.

Experimental Procedures

Equipment and reagents – The Biacore 3000 apparatus, CM4 sensor chips, amine coupling kit and HBS-P buffer (10 mM HEPES, 150 mM NaCl, 3 mM EDTA, 0.005% surfactant P20, pH 7.4) were from Biacore AB. Biotin-LC-hydrazide was from Pierce. Streptavidin, 6 kDa HP, and 35-45 kDa chondroitin 4 sulfate (CS-A, here abbreviated CS) were from Sigma, streptavidin-Cy5 or -Cy3 was from Amersham, and 9 kDa HS was from Celsus. Concerning the 6 kDa HP, smaller molecular species that this material may contain were removed through a filtration column. This material was routinely used for Biacore analysis (18). This material was preferred to unfractionated heparin because it is less polydisperse. CS-A contains on average one sulfate group by disaccharide. The

molecular weight of the HS used in this study was 9000 g/mol as determined by sedimentation-diffusion analysis. Its S and N contents, determined by elemental analysis, were 6.96 and 2.15%, respectively (Georges Pavlov and Christine Ebel, personal communication). Lysotracker red DND-99 and Alexafluor® 488 or 594-conjugated transferrin are from InVitrogen. Size-defined HP-derived oligosaccharides (dp6, hexa-; dp12, dodeca-; and dp18, octadeca-saccharide) were prepared from porcine mucosal HP as described (19). These HP-derived oligosaccharides were obtained by size fractionation. Because starting material is HP, and HS, these samples are relatively homogenous and highly sulfated. Strong anion exchange HPLC analysis of the HP-derived octasaccharide gives rise to three major picks.

MCa, MCa_b, MCa K20A and MCa_b K20A peptide syntheses – Chemical syntheses of MCa and MCa K20A or biotinylated MCa_b and MCa_b K20A were performed as previously described (2,6). The molecular weights of the peptides are 3858.62 (MCa) and 3801.52 (MCa K20A). Their pI values are 9.46 (MCa) and 9.30 (MCa K20A) indicating that they are basic at physiological pH 7.4. Primary structures of MCa and MCa K20A are shown in Figure 1A. The position of biotin in MCa_b and MCa_b K20A are on an extra N-terminal lysine residue.

Formation of MCa_b- or MCa_b K20A-Strep-Cy5/3 complexes – Soluble streptavidin-Cy5 or –Cy3 (Amersham) was mixed with four molar equivalents of MCa_b or MCa_b K20A for 2 hrs at 37°C in the dark in phosphate-buffered saline (PBS, in mM): NaCl 136, Na_2HPO_4 4.3, KH_2PO_4 1.47, KCl 2.6, $CaCl_2$ 1, $MgCl_2$ 0.5, pH 7.2. In some experiments, where indicated, various molar ratios of MCa_b and streptavidin-Cy3 were used to prepare the MCa_b-Strep complex, the concentration of streptavidin-Cy3 being kept constant (1 µM).

Surface plasmon resonance binding experiments – 6 kDa HP and HS were biotinylated at their reducing end with Biotin-LC-Hydrazide. The biotinylation procedure was checked by streptavidin-peroxydase labeling after blotting of the material onto zetaprobe membrane. These molecules have been widely used to study HP or HS binding onto several other proteins, such RANTES, IFNg, gp120 or CXCL12 (18,20-22). For the purpose of immobilization of biotinylated HP and HS on a Biacore sensorchip, flow cells of a CM4 sensorchip were activated with 50 µl of 0.2 M N-ethyl-N'-(diethylaminopropyl)-carbodiimide and 0.05 M N-hydroxysuccinimide before injection of 50 µl of streptavidin (0.2 mg/ml in 10 mM acetate buffer, pH 4.2). Remaining activated groups were blocked with 50 µl ethanolamine 1 M, pH 8.5. Typically, this procedure permitted coupling of approximately 3.000-3.500 resonance units (RU) of streptavidin. Biotinylated HP (5 µg/ml) or HS (10 µg/ml) in HBS-P buffer was then injected over one surface flow cell to obtain an immobilization level of approximately 50 RU. Flow cells were then conditioned with several injections of 2 M NaCl. One flow cells was left untreated and served as negative control. For binding assays, different MCa concentrations in HBS-P and at 25°C were simultaneously injected at 20 µl/min onto the control, HP and HS surfaces during 5 min, after which the formed complexes were washed with running buffer. The sensorchip surfaces were regenerated with a 5 min pulse of 2 M NaCl in HBS-P buffer. For competition assays, MCa at 2 µM was preincubated for at least 45 min with various molar excesses of HP-derived oligosaccharides (dp6, dp12, and dp18), and then injected over the HP surface as described above.

Cell culture and transfection – Wild-type Chinese Hamster Ovary (CHO-K1) cell line and mutant CHO cell lines lacking all GAGs (pgsB-618) or HS (pgsD-677) (ATCC) were maintained at 37°C in 5% CO_2 in F-12K nutrient medium (InVitrogen) supplemented with 10% (v/v) heat-inactivated fetal bovine serum (InVitrogen) and 10,000 units/ml streptomycine and penicillin (InVitrogen). For transfection experiments with Fugene® HD (Roche), wild-type and mutant pgsB-618 CHO cells were transfected with a plasmid that encodes a dominant-negative form of dynamin 2 (dynamin 2 K44A) in fusion with EGFP (pEGFP-N1 vector from Clontech). 24 hrs following transfection, cells were incubated with 1 µM MCa_b-Strep-Cy3 or transferrin-conjugated to Alexafluor-594 (25 µg/ml).

Flow cytometry – MCa_b/ MCa_b K20A-Strep-Cy5 complexes were incubated for 2 hrs in phosphate

buffered saline with CHO and mutant cells to allow cell penetration. The cells were then washed twice with PBS to remove the excess extracellular complexes. Next, the cells were treated with 1 mg/ml trypsin (InVitrogen) for 10 min at 37°C to remove remaining membrane-associated extracellular cell surface-bound complexes. After trypsin incubation, the cell suspension was centrifuged at 500 g and suspended in PBS. For inhibition studies, MCa_b-Strep-Cy5 complexes were preincubated with PBS containing variable concentrations (as indicated) of CS-A, HP or HS for 45 min, and the mixture incubated with cells for 2 hrs to investigate cell penetration. Washing and trypsination steps were also applied in these conditions. For experiments concerning endocytosis inhibitors, wild-type and mutant CHO cells were initially washed with F12K, and preincubated for 30 min at 37° C with different inhibitors of endocytosis: (i) 5 mM amiloride, (ii) 5 µM cytochalasin D, (iii) 5 mM nocodazole, or (iv) 5 mM methyl-β-cyclodextrin (all from Sigma). The cells were then incubated for 2 hrs at 37°C with 1 µM MCa_b-Strep-Cy5 or with 25 µg/ml transferrin-Alexafluor 488 in presence of each drug. For all these experimental conditions, flow cytometry analyses were performed with live cells using a Becton Dickinson FACSCalibur flow cytometer (BD Biosciences). Data were obtained and analyzed using CellQuest software (BD Biosciences). Live cells were gated by forward/side scattering from a total of 10,000 events.

Confocal microscopy - For analysis of the subcellular localization of MCa_b-Strep-Cy5 complexes in living cells, CHO and mutant cells were incubated with the complexes for 2 hrs, and then washed with DMEM alone. Immediately after washing, the nucleus was stained with 1 µg/ml dihydroethidium (DHE, Molecular probes, USA) for 20 min, and then washed again with DMEM. After this step, the plasma membrane was stained with 5 µg/ml FITC-conjugated concanavalin A (Sigma) for 3 min. Cells were washed once more, but with PBS. Live cells were then immediately analyzed by confocal laser scanning microscopy using a Leica TCS-SP2 operating system. FITC (E_x=488 nm), Cy5 (E_x= 642 nm) or Cy3 (E_x= 543 nm) fluorescence emission were collected in z-confocal planes of 10-15 nm. Images were merged in Adobe Photoshop 7.0. For studies on endocytosis, wild-type and mutant CHO cells were incubated with 1 µM MCa_b-Strep-Cy5 along with 25 µg/ml transferrin conjugated to Alexafluor-488 (a marker of clathrin-mediated endocytosis) for 2 hrs and the distribution was analysed through confocal microscopy. In parallel studies, cells were first incubated for 2 hrs with 1 µM MCa_b-Strep-Cy5, washed with PBS and incubated with 50 nM lysotracker red DND-99 for 20 min at 37°C. Cells were then washed again with PBS and visualized alive by confocal microscopy.

Effect of HP on the interaction of MCa_b with lipids - Strips of nitrocellulose membranes containing spots with different phospholipids and sphingolipids were obtained from Molecular Probes. These membranes were first blocked with TBS-T (150 mM NaCl, 10 mM Tris-HCL, pH 8.0, 0.1% (v/v) Tween 20) supplemented with 0.1% free bovine serum albumin (BSA) for about 1 hr at room temperature and then incubated for 2 hrs at room temperature in TBS-T 0.1% free BSA with either 100 nM MCa_b alone or a MCa_b/HP complex, resulting from a 45 min pre-incubation of 100 nM MCa_b with 10 µg/ml HP. Incubation of the membranes with 100 nM biotin alone was used as a negative control condition. The membranes were then washed a first time with TBS-T 0.1% free BSA using a gentle agitation for 10 min. In all conditions, MCa_b or biotin binding onto the lipid spots was detected by a 30 min incubation with 1 µg/ml streptavidin horse radish peroxidase (Vector labs, SA-5704), followed by a second wash with TBS-T 0.1% free BSA, and an incubation with horse radish peroxidase substrate (Western Lightning, Perkin-Elmer Life Science) for 1 min. Lipid membranes were then exposed to a Biomax film (Kodak). The intensity of interaction with the lipids was analyzed with Image J (National Institute of Health, USA).

Results

MCa interacts with HS and HP - Pre-incubation of MCa_b with HP was found to partially inhibit its penetration in HEK293 cells (5). To evaluate the binding of MCa to HSPGs, HP or HS were coupled to a Biacore sensorchip and the MCa binding monitored by SPR (Figure 1). Injection of a range of MCa concentrations (up to 5 µM) over

HP- or HS-coupled sensorchips gave rise to increasing binding amplitudes as shown in Figure 1B. A mutated analogue of MCa (MCa K20A) showed impaired binding activity, indicating the importance of residue K20 for glycosaminoglycan recognition. This finding is in agreement with the role of HSPGs in the cell entry of CPPs and with the observation that the MCa K20A has impaired cell penetration (6). The data could not be fitted to a binding model, presumably because all binding curves had a "square" shape with sharp edges, suggesting high association and dissociation rates. We were thus not able to extract reliable kinetic values from curve fitting. Equilibrium data, plotted according to the Scatchard representation, were used to determine affinity (Figure 1C). The straight lines obtained show that MCa recognizes a single class of binding site, characterized by an affinity constant of K_d = 2.1 µM (HP) or 4.6 µM (HS). Since HP (6 kDa) and HS (9 kDa), immobilized at a level of 55 and 45 RU, respectively, both permitted a maximun binding of 155 RU of MCa (3859 Da), we calculated that each HP molecule bound an average of 4.4 MCa and each HS molecule bound an average of 8 MCa. These two molecules contain, respectively, an average of 20 and 36 saccharidic units (using an approximative MW of 600 for the HP-derived disaccharides, and 500 for the HS-derived disaccharides), thus it can be estimated conversely that each MCa should occupy, in both cases, an average of 4.5 monosaccharide units (20/4.4 or 36/8) along the GAG chain.

HP is formed by the polymerization of a various number of disaccharide units. In order to study the effect of the size of the polymer on its interaction with MCa, we performed competition experiments using HP-derived oligosaccharides of defined degree of polymerization (dp) (Figure 1D). For this purpose, wild-type MCa was pre-incubated with different HP-derived oligosaccharides (dp6, dp12 or dp18), as mentioned in the *Materials and Methods*, and then injected over the HP-conjugated sensorchip. As shown, the oligosaccharides caused a dose-dependent inhibition of the interaction of MCa with HP. dp18 was the most active oligosaccharide with an IC_{50} close to 1 µM. In contrast, dp6 had almost no effect at 5 µM.

Dose-dependent penetration of MCa_b-Strep-Cy5 in wild-type and mutant CHO cell lines - Results presented in Figure 1 indicate that MCa interacts with negatively charged HP and HS. To challenge the implication of HP and HS in the cell penetration of MCa, the cell penetration efficacy of MCa_b-Strep-Cy5 was assessed using wild-type CHO cells (CHO wild-type) and mutant CHO cells lacking either HS (CHO pgsD-677) or all GAGs (CHO pgsB-618). Each CHO cell lines were incubated for 2 hrs in the presence of variable concentrations of MCa_b-Strep-Cy5 complexes, and the amount of internalized complex was measured by FACS. Figure 2A represents the dose-response curves for MCa_b-Strep penetration in the three CHO cell lines. Half saturation of MCa penetration (PC_{50}) was only slightly modified by the absence of GAG, PC_{50} of 0.46 µM, 0.56 µM and 0.71 µM in CHO wild-type, CHO pgsD-677 and CHO pgsB-618, respectively**.** In contrast the maximum amount of incorporated MCa_b-Strep-Cy5, measured in the presence of 1 µM of complex, was strongly reduced in both the pgsD-677 and pgsB-618 CHO lines compared to the wild-type CHO, 43.0 ± 3.0% (n=3) and 57.0 ± 2.5% (n=3) reduction in pgsD-677 and pgsB-618 CHO respectively (Figure 2B). Similar experiments were done using the mutant MCa_b K20A that has been previously shown to exhibit reduced penetration compared to the wild-type MCa (6). Results presented on Figure 2B shows that although already strongly reduced in wild-type CHO, the penetration of this mutant was further reduced in the HS- or GAGs-deficient CHO resulting in similar reductions in cell entry, 45 ± 2% (n=3) and 60 ± 4% (n=3) reduction in pgsD-677 and pgsB-618 CHO, respectively. This result indicates that the mechanism of cell penetration of the K20A mutant is identical to that of wild-type MCa, in spite of the reduction in cell entry induced by the mutation. Therefore, MCa_b K20A also relies on GAG-dependent and GAG-independent mechanisms for cell penetration. This observation is consistent with the fact that the K20A mutation in MCa only reduces the PC_{50} value (6). In addition, the significant amount of MCa_b-Strep-Cy5 taken up by GAG-deficient cells indicates that a significant fraction of MCa_b-Strep-Cy5 penetration is GAG-independent, likely relying on the contribution of plasma membrane lipids.

Inhibition of cell penetration of MCa_b-Strep-Cy5 by soluble HSPGs – According to the two

observations described above, (i) interaction of MCa with HSPGs and (ii) reduction in MCa cell penetration in GAG-deficient cells, one would expect that incubation of MCa with soluble GAGs also reduce the penetration of MCa_b-Strep-Cy5. To challenge this point, MCa_b-Strep-Cy5 was pre-incubated with various concentrations of HS, HP or CS for 45 min, before incubation with wild-type or GAG-deficient CHO cells for 2 hrs. Total amount of MCa_b-Strep-Cy5 inside the cell was then measured by flow cytometry (Figure 3). In wild-type CHO cells, HS (250 µg/ml) produced the most potent inhibition of cell penetration (84 ± 2%, n=3, Figure 3A). HP and CS were less efficient than HS with a mean inhibition of 59 ± 10% (n=3) and 19 ± 2% (n=3) for HP and CS, respectively (at 250 µg/ml). Linking inhibition with the global negative charge of the GAG tested remains hazardous because charge relationship follows the rule HP > CS > HS, and here we observe CS>HP>HS. Interestingly, all three GAGs also reduced the cell penetration of MCa_b-Strep-Cy5 in GAG-deficient cells with the same rank as observed for wild-type CHO cells (Figure 3B). Incubation of MCa_b-Strep-Cy5 with HS, HP or CS induced a significant inhibition in GAG-deficient cells (61 ± 9% (n=3), 45 ± 4% (n=3), and 10 ± 1% (n=3) in the presence, respectively, of 250 µg/ml HS, HP and CS) although lower than in wild-type CHO cells. Therefore, these data indicate that binding of soluble GAGs to MCa inhibit the cell penetration of MCa_b-Strep-Cy5 not only by preventing its interaction with CHO cell surface GAGs, but also with non-GAG cell surface components.

To check whether GAGs could inhibit the interaction of MCa with membrane lipids, we investigated the effect of HP on MCa_b interaction with lipids immobilized on strips (Figure 4A). MCa_b (100 nM) was incubated for 45 min in the presence or absence of HP (10 µg/ml) before incubation with lipid strips,as described under *Materials and Methods*. As shown in Figure 4, HP significantly decreased the interaction of MCa_b with phosphatidic acid (66%), sulfatide (30%), Ptdlns(4)P (31%), Ptdlns(3,4)P_2 (26%) and Ptdlns(3,4,5)P_3 (72%), but not with lipids such as Ptdlns(3)P, Ptdlns(5)P or Ptdlns(3,4,5)P_2. These results provide a clear explanation of the fact that the interaction of MCa_b with soluble GAGs may also lead to an inhibition of the GAG-independent MCa_b cell penetration.

Effect of HSPGs on the cell distribution of MCa_b-Strep-Cy5 – In order to examine the contribution of cell surface GAGs to the cell distribution of MCa_b-Strep-Cy5, MCa_b-Strep-Cy5 localization within the cell was defined using confocal microscopy and compared between wild-type and GAG-deficient CHO cell lines. For these experiments, the plasma membrane, the nucleus and MCa_b-Strep were labeled with concanavaline A (green), DHE (red) and Cy5 (blue), respectively. Images presented on Figure 5 were obtained 2 hrs after the start of the cell incubation. Living cells were used in order to avoid possible cell distribution artifacts that may occur during the fixation procedure (5,9,23)**.** As shown, MCa_b coupling to Strep-Cy5 is required for the cell penetration of Strep-Cy5 into CHO cells (Figure 5A). The MCa_b-Strep-Cy5 complex is exclusively present as punctuate dots in the cytoplasm of living CHO cells. A similar cell distribution is observed in living CHO cell mutants lacking just HS (pgsD-677) or all GAGs (pgsB-618) suggesting that GAG-dependent and GAG-independent cell entries produce similar cell distributions (Figure 5B). A Strep-Cy5 complex made with the MCa_b K20A analogue produces a similar subcellular distribution than MCa_b-Strep-Cy5 in wild-type and HS-deficient CHO cells, suggesting that the mechanism of cell penetration is not altered by point mutation of MCa_b (data not shown). Punctuate staining of MCa_b-Strep-Cy5 is indicative of a form of endosomal localization. This point was further investigated.

MCa_b-Strep-Cy5 localizes to endosomal structures that do not originate from clathrin-mediated endocytosis – Using confocal microscopy, the cell distribution of MCa_b-Strep-Cy5 was compared to that of endosomal structures as revealed by lysotracker red staining. As shown on Figure 6A there is a very good co-localization between MCa_b-Strep-Cy5 and lysotracker red fluorescence in all cell lines used (CHO wild-type, CHO pgsB-618, and CHO pgsD-677). These data clearly indicate that the lack of GAGs does not alter the subcellular localization of MCa_b-Strep-Cy5, suggesting that both GAG-dependent and GAG-independent cell penetration rely on endocytosis. In order to

determine whether the type of endocytosis involved in MCa_b-Strep-Cy5 entry could be altered in GAG-deficient cells, we first analyzed whether it had common features with clathrin-mediated endocytosis. Transferrin is known to enter cells via transferrin receptors through clathrin-mediated endocytosis (24,25). As shown here, there was an almost complete absence of co-localization between MCa_b-Strep-Cy5 and transferrin-labeled with Alexafluor-488 in wild-type as well as in mutant CHO cells (Figure 6B). These data indicate that the route of entry of Strep-Cy5, when coupled to MCa_b, is not through clathrin-mediated endocytosis. It also indicates that the absence of GAGs at the cell surface does not favor clathrin-dependent endocytosis for the cell entry of MCa_b-Strep-Cy5 over other mechanisms of endocytosis.

Expression of a dominant-negative mutant of dynamin 2, dynamin 2 K44A, is known to prevent normal clathrin-mediated endocytosis (26). As shown in Figure 7A, expression of dynamin 2 K44A prevents the entry of transferrin-alexafluor-594 in both wild-type and GAG-deficient CHO cells confirming that transferrin receptors get internalized by clathrin-mediated endocytosis. In contrast, MCa_b-Strep-Cy3 entry was not prevented by the expression of dynamin 2 K44A (Figure 7B), clearly indicating that clathrin-mediated endocytosis was not required for the entry of MCa_b when coupled to streptavidin.

Lack of alteration of the main endocytosis entry pathway in GAG-depleted cells - To further identify the route of entry of MCa_b-Strep-Cy5 and analyze the impact of GAG depletion on this process, several inhibitors were tested by FACS on the entry of MCa_b-Strep-Cy5 in wild-type (Figure 8A) and pgsB-618 CHO cells (Figure 8B). These inhibitors were also tested on the entry of transferrin-Alexafluor-488 for comparison. Amiloride was tested to block macropinocytosis, methyl-β-cyclodextrin to deplete membrane cholesterol and inhibit lipid raft-dependent pathways, nocodazole to inhibit microtubule formation, and cytochalasin D to inhibit F-actin elongation, required for macropinocytosis and clathrin-dependent endocytosis (27). Chlorpromazine, an inhibitor of clathrin-mediated endocytosis could not be tested because it produced cell dissociation from the plastic dish surface (data not shown). In wild-type CHO cells, transferrin-Alexafluor-488 endocytosis is not affected by amiloride, methyl- β-cyclodextrin or nocodazole, as expected for clathrin-mediated endocytosis. Cytochalasin D was found to produce a curious 37% increase in the cell entry of transferrin indicating an alteration in clathrin-dependent endocytosis. In contrast, with the exception of methyl-β-cyclodextrin, all drugs tested were found to inhibit partially the entry of MCa_b-Strep-Cy5 in wild-type CHO cells (Figure 8A). The lack of effect of methyl-β-cyclodextrin indicates that caveolae-mediated endocytosis is not involved in the entry of MCa_b-Strep-Cy5. The fact that both amiloride and cytochalasin D inhibit MCa_b-Strep-Cy5 cell entry by 80% and 30%, respectively, indicates a significant contribution of macropinocytosis pathway. Cytochalasin D probably acts exclusively on macropinocytosis for the cell entry of MCa_b-Strep-Cy5 since the involvement of the other major endocytic pathway affected by this drug, clathrin-mediated endocytosis, can be ruled out. Nocodazole, which has a wide range of effects on various endocytosis pathways, had also a great effect, inducing a 63% reduction of MCa_b-Strep-Cy5 cell entry. Thus, the rather segregated effects of endocytosis inhibitors on cell penetration of transferrin and MCa_b-Strep-Cy5 is coherent with their lack of colocalization inside cells (Figure 6B). These data stress the importance of macropinocytosis as the main entry pathway of Strep-Cy5 when coupled to MCa_b. The same set of drugs was then tested for the cell entry of both transferrin and MCa_b-Strep-Cy5 in GAG-deficient pgsB-618 CHO cells (Figure 8B). Interestingly, in the absence of GAGs, the effects of the endocytosis inhibitors on MCa_b-Strep-Cy5 entry were not altered indicating that in the absence of cell surface GAGs, macropinocytosis is still the main route of entry of the complex. This is in perfect agreement with the data shown in Figures 5 & 6, suggesting similar cell distribution of the complex, colocalization with lysotracker red and identical effects of dynamin 2 K44A expression. Surprisingly, the absence of GAGs had an impact on the effects of the drugs on transferrin entry (Figure 8B). Although no clear explanation can be provided for this observation, it may suggest that in the absence of GAGs, inhibition of alternative endocytosis pathways favors somehow clathrin-mediated endocytosis. These effects

remain however outside the focus of this study, namely the entry pathways of MCa, but are clear indications of the potential importance of GAGs in endocytosis.

The molar ratio MCa_b / Strep-Cy3 does not influence the type of endocytosis – Streptavidin molecules are tetramers that can bind up to four MCa_b peptides. It is therefore possible that the number of bound peptides may somehow affect the residency time of the complex at the cell surface and influence thereby the mode of cell penetration. To test this hypothesis, various molar ratios of MCa_b and Strep-Cy3 were mixed together in order to prepare complexes with increased numbers of MCa_b immobilized on Strep-Cy3. The exact molar ratio between MCa_b and Strep-Cy3 can however not be warranted by simply mixing various molar ratios of the two molecules. Once these complexes were prepared, their cell entry, along with the effect of amiloride, were quantified by FACS (Figure 9). Increasing the molar ratio of MCa_b over Strep-Cy3 from 1:1 to 8:1 dramatically increases the amount of Strep-Cy3 that penetrates into wild-type CHO cells (Figure 9A). These data indicate that immobilizing an increasing number of MCa_b onto streptavidin greatly favors the entry of the complex, possibly by multiplying the number of contacts with cell surface components and/or increasing the residency time at the cell surface. In contrast, using increased amounts of non-biotinylated MCa, unable to bind Strep-Cy3, in place of MCa_b, did not produce any increase in Strep-Cy3 penetration indicating that coupling of MCa to Strep-Cy3 was required (Figure 9B). This result also shows that the association of MCa to cell surface components does not trigger a generalized increase in cell endocytosis that would indirectly favor the penetration of MCa_b-Strep-Cy3 complexes. Finally, Figure 9C indicates that coupling several MCa_b peptides to streptavidin does not quantitatively alter the effect of 5 mM amiloride, indicating that macropinocytosis remains the predominant mode of entry of the complex regardless of the MCa_b / Strep-Cy3 molar ratio used.

Discussion

HSPGs are new cell surface targets of MCa that are involved in cell penetration of this peptide – Using a Biacore system, we have demonstrated that MCa, a member of a new family of CPPs, directly interacts with HP and HS with affinities in the low micromolar range (between 2 and 5 µM). These values are more or less well correlated to the PC_{50} values of MCa_b-Strep-Cy5 in CHO cells (around 0.5 µM) suggesting a contribution of HSPGs to the cell penetration of this complex. This slight difference could be related to the fact that each streptavidin molecule has the ability to bind four MCa molecules, thereby increasing the local concentration of the CPP in the vicinity of the cell surface receptors. Indeed, we show here that, increasing the molar ratio of MCa_b over streptavidin during complex formation produces an increase in cell penetration efficiency. Alternatively, differences may also be related to the exact nature of the cell surface HSPG involved in MCa interaction. By using HS- and GAG-deficient CHO cell lines, we conclusively demonstrate that HSPGs quantitatively contribute to more than 57% of the cell entry of Strep-Cy5 when coupled to MCa. HS represents the most important GAG since it is responsible for 75% of the GAG contribution. However, since a significant fraction of the total cell entry is conserved in GAG-deficient cells, the entry of MCa_b-Strep-Cy5 does not solely rely on GAGs, but also on other cell surface components, with apparent affinities closely related to that of MCa for HSPGs since the PC_{50} values varied only mildly in GAG-deficient CHO cells. Data presented here and in previous manuscripts (5,6) indicate that membrane lipids are also cell surface receptors for MCa. For instance, MCa was found to interact with the ganglioside GD3 with a closely related apparent affinity of 0.49 µM. Another important conclusion that can be made from these data is that the increase or the decrease of the penetration efficiency observed with specific mutants of MCa, such as MCa K20A tested herein, results from a modification of the apparent affinity of these MCa mutants for the cell surface components with which they interact. For instance, MCa K20A was found to have reduced apparent affinity for both HS and HP (present data) but also for membrane lipids (6). There is thus an interesting parallel to pursue on the structural determinants of CPP interaction with HSPGs and negatively charged lipids that may ultimately result in the design of better CPP analogues. This

observation appears particularly pertinent since the cell entry process of MCa-Strep-Cy5 or MCa-Strep-Cy3 complex, i.e. macropinocytosis, seems independent of the type of membrane receptor involved in MCa binding (HSPGs *versus* lipids).

HP inhibition of the cell penetration of MCa-Strep complex is not limited to the interaction of this CPP to cell surface HSPGs - HP-induced inhibition of CPPs cell entry is generally interpreted as being due to an inhibition of CPP interaction with cell surface HSPGs (28). However, an alternative possibility is that, by neutralizing the basic face of MCa, the interaction of HP with MCa also inhibits the subsequent interaction of MCa with negatively charged lipids of the cells, another surface component for the route of entry of MCa. Three sets of evidence indicate that this interpretation is likely to be correct. First, both soluble HS and HP inhibit the cell entry of MCa_b-Strep-Cy5 to levels beyond that measured for MCa_b-Strep-Cy5 entry in HS- and GAG-deficient CHO cells. Second, soluble HS and HP still produce significant reductions of MCa_b-Strep-Cy5 entry in GAG-deficient CHO cells, clearly indicating an inhibition through an alternate mode of inhibition. Third, incubation of HS with MCa_b produces a reduction in the interaction of MCa_b with several negatively charged lipids, the most dramatic effects being observed for PtdIns(3,4,5)P_3 and phosphatidic acid. These observations indicate that interpretation of the involvement of cell surface HSPGs in the penetration of CPPs based on soluble HP inhibition should be performed carefully. They also confirm the importance of the basic face of CPPs in the mechanism of cell penetration. Finally, the presence of a residual MCa-Strep complex penetration in GAG-deficient CHO cells in the presence of HS or HP might indicate that either the interaction between HSPGs is rapidly reversible or that this interaction does not fully cover the entire molecular surface of MCa required for cell penetration. Further detailed biochemical experiments will be needed to sort out the molecular determinants of MCa involved in HP or HS interaction. Such an investigation will determine to what extent the basic surface of MCa is involved in an interaction with HSPGs.

Macropinocytosis is the main endocytic pathway used by MCa when coupled to streptavidin in GAG-positive and GAG-deficient CHO cells – In a previous work, we reported that MCa-Strep complex penetration in HEK 293 cells was also observed in the presence of amiloride or nystatin suggesting that a non-endocytic pathway was involved in the penetration process (4). Here, we provide a quantitative analysis of the effects of endocytosis inhibitors on the entry of MCa_b-Strep-Cy5 in CHO cells using a FACS method and show that endocytosis represents the major route of penetration, while only 20 % of MCa_b-Strep-Cy5 penetration is still observed in the presence of endocytosis inhibitors (amiloride). Interestingly, the amount of MCa_b-Strep-Cy5 taken up in the presence of amiloride is close to the amount of complex taken up in GAG-deficient CHO cells in the presence of HS or HP. The apparent discrepancy between the two studies is likely due to the fact that confocal analysis used in the previous work was not quantitative enough to allow the calculation of the relative importance of each mechanism. Moreover, we cannot rule out the possibility that some endocytosis pathway, insensitive to amiloride or nystatin, may be present in the previously studied HEK293 cell line. This indicates that one needs to be cautious with regard to confocal images that are unfortunately not quantitative enough to rule out one or several cellular mechanisms for cell entry. Use of a marker of endosomes demonstrates that MCa_b-Strep-Cy5 is distributed within endosomes after cell entry, supporting the fact that endocytosis is a predominant route of entry of the cargo when coupled to MCa_b. The total lack of co-localization between transferrin-Alexafluor 488 and MCa_b-Strep-Cy5 clearly indicates that clathrin-mediated endocytosis is not at play in the entry of MCa_b-Strep-Cy5. This was further proven by i) the lack of effect of expression of dynamin 2 K44A, a dominant negative construct that inhibits clathrin-mediated endocytosis but does not prevent MCa_b-Strep-Cy3 entry, and ii) the differential effects of various endocytosis blockers on transferrin-Alexafluor 488 and MCa_b-Strep-Cy5 cell entries. The effects of cytochalasin D and of amiloride indicate that macropinocytosis is predominantly involved in the cell entry of MCa_b-Strep-Cy5. This observation is consistent with many other reports that indicate a role of macropinocytosis in cell

entry of other CPPs (14,29). However, the lack of effect of methyl-β-cyclodextrin appears to indicate that endocytosis of MCa_b-Strep-Cy5 is not dependent on lipid rafts or at least on cholesterol availability. Since macropinocytosis appears to be responsible for the uptake of MCa_b-Strep-Cy5/3 in wild-type and GAG-deficient CHO cells alike, it seems that all surface components able to bind MCa, negatively-charged HSPGs and lipids, are involved in macropinocytosis. Owing to the nature of macropinosomes, that do not fuse with lysosomes and that are leaky, it is likely that release of CPPs in the cytosol may occur very slowly. In the case of the Strep-Cy5 cargo, this leakage was however not observed when coupled to MCa_b.

Cargo-dependence of MCa mode of penetration and/or release in the cytosol? – The mechanism of cell penetration of CPPs remains highly debated. There are pro and con arguments in favor of membrane translocation, a process whereby the peptide would flip from the outer face of the plasma membrane to the inner face, then released free into the cytoplasm. Here, we do not provide compelling evidence for a translocation mechanism for Strep-Cy5 entry when coupled to MCa_b. On the contrary, the data strongly emphasizes the importance of endocytosis in the penetration of the vector/cargo complex. Nevertheless, the issue of the mode of penetration of MCa itself remains open to a large extent. First, there is compelling evidence that MCa has a near-complete pharmacological effect when applied at the extracellular face of cells. Second, the pharmacological site of MCa on the ryanodine receptor has been localized to the cytosol face of the calcium channel. Taken together, these results suggest that MCa must reach the cytosol within seconds or minutes. Two possibilities can be envisioned: (i) MCa may be released within the cytosol from leaky macropinosomes immediately after uptake but the time scale seems inappropriate, or (ii) when "free", i.e. not coupled to a cargo, MCa may indeed simply translocate through the membrane. This raises immediately the question of the contribution of the cargo to the mode of entry of MCa. Streptavidin is a cargo that can bind four different MCa_b molecules. Linking multiple vectors to a single cargo molecule could theoretically complicate the mode of entry of MCa. Intuitively, one could imagine that multiple attachment points to cell surface components might hamper the translocation of the peptide through the plasma membrane, increase the residency time at the cell surface, and thereby strongly promote macropinocytosis over direct translocation. Experimentally, this is however not observed. The fact that amiloride inhibits penetration of MCa_b-Strep-Cy5 complex, prepared with 1 MCa_b for 1 Strep-Cy5, as efficiently as the penetration of MCa_b-Strep-Cy5 complex, prepared with 8 MCa_b for 1 Strep-Cy5, indicates that macropinocytosis is not influenced by the presence of multiple MCa_b molecules. Therefore the putative difference between "free" MCa_b and MCa_b-cargo complex might be due to the nature of the cargo rather than its specific properties of MCa_b binding. In addition, the size of the cargo may itself represent a problem for simple diffusion of the complex from "leaky" macropinosomes to the cytosol. Further studies will be required to investigate the contribution of cargo size and nature in the mode of entry and cell distribution (cytosol *versus* endosomes) of the vector. Nevertheless, these data are coherent with many other studies on CPPs and macropinocytosis is likely to be the main entry route of many other cargoes that will be attached to maurocalcine. Although streptavidin is used as a reporter cargo here (fluorescence property), it is worth mentioning that its ability to bind to several different biotinylated molecules at a time should be considered as a significant advantage for the cell delivery of multiple cargoes with a single MCa vector.

REFERENCES

1. Mosbah, A., Kharrat, R., Fajloun, Z., Renisio, J. G., Blanc, E., Sabatier, J. M., El Ayeb, M., and Darbon, H. (2000) *Proteins* **40**, 436-442
2. Esteve, E., Smida-Rezgui, S., Sarkozi, S., Szegedi, C., Regaya, I., Chen, L., Altafaj, X., Rochat, H., Allen, P., Pessah, I. N., Marty, I., Sabatier, J. M., Jona, I., De Waard, M., and Ronjat, M. (2003) *J Biol Chem* **278**, 37822-37831
3. Chen, L., Esteve, E., Sabatier, J. M., Ronjat, M., De Waard, M., Allen, P. D., and Pessah, I. N. (2003) *J Biol Chem* **278**, 16095-16106
4. Esteve, E., Mabrouk, K., Dupuis, A., Smida-Rezgui, S., Altafaj, X., Grunwald, D., Platel, J. C., Andreotti, N., Marty, I., Sabatier, J. M., Ronjat, M., and De Waard, M. (2005) *J Biol Chem* **280**, 12833-12839
5. Boisseau, S., Mabrouk, K., Ram, N., Garmy, N., Collin, V., Tadmouri, A., Mikati, M., Sabatier, J. M., Ronjat, M., Fantini, J., and De Waard, M. (2006) *Biochim Biophys Acta* **1758**, 308-319
6. Mabrouk, K., Ram, N., Boisseau, S., Strappazzon, F., Rehaim, A., Sadoul, R., Darbon, H., Ronjat, M., and De Waard, M. (2007) *Biochim Biophys Acta* **1768**, 2528-2540
7. Derossi, D., Calvet, S., Trembleau, A., Brunissen, A., Chassaing, G., and Prochiantz, A. (1996) *J Biol Chem* **271**, 18188-18193
8. Suzuki, T., Futaki, S., Niwa, M., Tanaka, S., Ueda, K., and Sugiura, Y. (2002) *J Biol Chem* **277**, 2437-2443
9. Vives, E., Richard, J. P., Rispal, C., and Lebleu, B. (2003) *Curr Protein Pept Sci* **4**, 125-132
10. Vives, E., Brodin, P., and Lebleu, B. (1997) *J Biol Chem* **272**, 16010-16017
11. Terrone, D., Sang, S. L., Roudaia, L., and Silvius, J. R. (2003) *Biochemistry* **42**, 13787-13799
12. Berlose, J. P., Convert, O., Derossi, D., Brunissen, A., and Chassaing, G. (1996) *Eur J Biochem* **242**, 372-386
13. Magzoub, M., and Graslund, A. (2004) *Q Rev Biophys* **37**, 147-195
14. Wadia, J. S., Stan, R. V., and Dowdy, S. F. (2004) *Nat Med* **10**, 310-315
15. Foerg, C., Ziegler, U., Fernandez-Carneado, J., Giralt, E., Rennert, R., Beck-Sickinger, A. G., and Merkle, H. P. (2005) *Biochemistry* **44**, 72-81
16. Sandgren, S., Cheng, F., and Belting, M. (2002) *J Biol Chem* **277**, 38877-38883
17. Nakase, I., Tadokoro, A., Kawabata, N., Takeuchi, T., Katoh, H., Hiramoto, K., Negishi, M., Nomizu, M., Sugiura, Y., and Futaki, S. (2007) *Biochemistry* **46**, 492-501
18. Laguri, C., Sadir, R., Rueda, P., Baleux, F., Gans, P., Arenzana-Seisdedos, F., and Lortat-Jacob, H. (2007) *PLoS ONE* **2**, e1110
19. Sadir, R., Baleux, F., Grosdidier, A., Imberty, A., and Lortat-Jacob, H. (2001) *J Biol Chem* **276**, 8288-8296
20. Vives, R. R., Imberty, A., Sattentau, Q. J., and Lortat-Jacob, H. (2005) *J Biol Chem* **280**, 21353-21357
21. Vives, R. R., Sadir, R., Imberty, A., Rencurosi, A., and Lortat-Jacob, H. (2002) *Biochemistry* **41**, 14779-14789
22. Sarrazin, S., Bonnaffe, D., Lubineau, A., and Lortat-Jacob, H. (2005) *J Biol Chem* **280**, 37558-37564
23. Richard, J. P., Melikov, K., Vives, E., Ramos, C., Verbeure, B., Gait, M. J., Chernomordik, L. V., and Lebleu, B. (2003) *J Biol Chem* **278**, 585-590
24. Kurten, R. C. (2003) *Adv Drug Deliv Rev* **55**, 1405-1419
25. Conner, S. D., and Schmid, S. L. (2003) *Nature* **422**, 37-44

26. Sun, T. X., Van Hoek, A., Huang, Y., Bouley, R., McLaughlin, M., and Brown, D. (2002) *Am J Physiol Renal Physiol* **282**, F998-1011
27. Mano, M., Teodosio, C., Paiva, A., Simoes, S., and Pedroso de Lima, M. C. (2005) *Biochem J* **390**, 603-612
28. Nascimento, F. D., Hayashi, M. A., Kerkis, A., Oliveira, V., Oliveira, E. B., Radis-Baptista, G., Nader, H. B., Yamane, T., Tersariol, I. L., and Kerkis, I. (2007) *J Biol Chem* **282**, 21349-21360
29. Rinne, J., Albarran, B., Jylhava, J., Ihalainen, T. O., Kankaanpaa, P., Hytonen, V. P., Stayton, P. S., Kulomaa, M. S., and Vihinen-Ranta, M. (2007) *BMC Biotechnol* **7**, 1

FOOTNOTES

*We thank Rabia Sadir for the kind preparation of oligosaccharides. We also thank Dr. McNiven MA for providing the cDNA encoding dynamin 2 K44A mutant. We acknowledge financial support of Inserm, Université Joseph Fourier and CEA for this project. Narendra Ram is a fellow of the Région Rhône-Alpes and is supported by an Emergence grant.

The abbreviations used are**:** BSA, bovine serum albumin; CHO, Chinese hamster ovary; CPP, cell penetrating peptide; CS, Chondroitine sulphate; DHE, dihydroethidium; DHPR, dihydropyridine receptor; DMSO, dimethyl sulfoxide; dp, degree of polymerisation; EDTA, ethylenediaminetetraacetic acid; FACS, fluorescence activated cell sorter; HEK293, human embryonic kidney 293 cells; HEPES, 4-(2-hydroxyethyl)-1-piperazineethanesulfonic acid; HSPG, heparan sulfate proteoglycans; ^{1}H-NMR, proton nuclear magnetic resonance; HP, Heparin; HS, Heparan sulphate; MCa, maurocalcine; MCa_b, biotinylated maurocalcine; PC_{50}, half-maximal penetration concentration; PBS, phosphate buffered saline; PtdIns, phosphatidylinositol; RyR, ryanodine receptor; SR, sarcoplasmic reticulum; Strep-Cy5 (Cy3), streptavidin-cyanine 5 (cyanine 3)

FIGURE LEGENDS

Fig. 1. Binding of wild-type MCa and MCa K20A to HP or HS immobilized on SPR sensorchip. (A) Primary structure of MCa and MCa K20A. Basic and acidic residues are in blue and red colors, respectively. The disulfide bridge patterns of both molecules are shown. (B) Sensorgrams of the interactions. Various concentrations of MCa or MCa K20A were injected over a HP- or HS-activated surface at a flow rate of 20 µl/min during 5 min. After this peptide injection time, running buffer was injected to monitor the wash off reaction. All responses were recorded and subtracted from the control surface online as a function of time (in response units, RU). Each set of sensorgrams was obtained with MCa at (from top to bottom) 5, 2.5, 1.25, 0.62, 0.31, 0.15 and 0 µM. (C) Scatchard plots of the equilibrium binding data measured on the sensorgrams corresponding to the injection of MCa over HP or HS SPR surfaces. Data were fitted with a linear equation of the type $y = a \times x + b$ where a = -0.46 (HP) or -0.22 (HS) and b = 82.5 (HP) or 33.7 (HS). Calculated binding affinities are Kd = 2.1 µM (HP) and Kd = 4.6 µM (HS). (D) Inhibition of the MCa/HP binding by HP-derived oligosaccharides. MCa (1 µM) was coincubated with increasing molar excess of dp6, dp12 or dp18 for 45 min, then injected over a HP-activated sensorchip for 5 min. Responses (in RU) were recorded and plotted as the percentage of maximum responses obtained without preincubation (70-80 RU).

Fig. 2. Cell penetration of MCa_b-Strep-Cy5 and MCa_b K20A-Strep-Cy5 in wild-type and HSPG mutant CHO cells. (A) Dose-dependent cell penetration of wild-type MCa_b-Strep-Cy5 in wild-type and mutant CHO cells), as assessed quantitatively by FACS. Representative experiment. The indicated concentrations are for streptavidin-Cy5 (from 10 nM to 2.5 µM). Data were fitted by a sigmoid equation

providing the following half effective concentrations PC_{50} = 0.46 ± 0.01 µM (wild-type CHO), 0.56 ± 0.01 µM (pgsD-677) and 0.71 ± 0.01 µM (pgsB-618). (B) Comparative cell penetration of 1 µM MCa_b-Strep-Cy5 and MCa_b K20A-Strep-Cy5 in CHO and CHO mutant cell lines. Representative experiment of n=3. Values are normalized with mean fluorescence intensity of wild-type CHO cells.

Fig. 3. Inhibition of MCa_b-Strep-Cy5 cell penetration by soluble GAGs in wild-type and GAG-deficient CHO cell lines. (A) Dose-dependent inhibition of MCa_b-Strep-Cy5 cell penetration by soluble GAGs in wild-type CHO cells. Representative experiment of n=3. Data were fitted by an hyperbola equation of the type $y = (a \times x) / (b + x)$ where a = 83.9 ± 1.7% (HS), 58.7 ± 9.8% (HP) and 18.7 ± 1.7% (CS), and b = 16.6 ± 1.2 µg/ml (HS), 29.1 ± 14.5 µg/ml (HP) and 1.8 ± 1.0 µg/ml (CS). (B) Dose-dependent inhibition of MCa_b-Strep-Cy5 cell penetration by soluble GAGs in GAG-deficient CHO cells. Representative experiment of n=3. Fitting values are a = 60.6 ± 8.6% (HS), 45.4 ± 3.5% (HP) and 9.8 ± 1.3% (CS), and b = 8.6 ± 2.0 µg/ml (HS), 46.2 ± 8.9 µg/ml (HP) and 3.3 ± 2.1 µg/ml (CS).

Fig. 4. Effect of HP on the interaction of MCa_b with membrane lipids. (A) 100 nM MCa_b alone, or MCa_b pre-incubated for 45 min with 10 µg/ml of HP, was incubated for 2 hrs with lipid strips. Each dot corresponds to 100 pmoles of lipid immobilized on the strip. Left panel: interaction with various sphingolipids. Numbers refer to: sphingosine (**1**), sphingosine 1-phosphate (**2**), phytosphingosine (**3**), ceramide (**4**), sphingomyelin (**5**), sphingosylphosphophocholine (**6**), lysophosphatidic acid (**7**), myriocin (**8**), monosialoganglioside (**9**), disialoganglioside (**10**), sulfatide (**11**), sphingosylgalactoside (**12**), cholesterol (**13**), lysophosphatidyl choline (**14**), phosphatidylcholine (**15**), and blank (**16**). Right panel: interaction with various phospholipids. The lipids are identified by their numbered positions on the strip (middle panel). Numbers refer to: lysophosphatidic acid (**1**), lysophosphatidylcholine (**2**), phosphatidylinositol (Ptdlns) (**3**), Ptdlns(3)P (**4**), Ptdlns(4)P (**5**), Ptdlns(5)P (**6**), phosphatidylethanolamine (**7**), phosphatidylcholine (**8**), sphingosine 1-phosphate (**9**), Ptdlns(3,4)P_2 (**10**), Ptdlns(3,5)P_2 (**11**), Ptdlns(4,5)P_2 (**12**), Ptdlns(3,4,5)P_3 (**13**), phosphatidic acid (**14**), phosphatidylserine (**15**), and blank (**16**). (B) Intensity of the interaction of MCa_b or MCa_b + HP with various lipids as analyzed by Image J (NIH). The data are quantified in arbitrary units and the results are presented as histograms. These experiments were repeated three times, data shown as triplicates. Significance is provided as a deviation of three times the SD value from 100% (denoted as asterisks).

Fig. 5. Cell distribution of MCa_b-Strep-Cy5 in living wild-type or mutant CHO cells. (A) Confocal images showing the cell penetration of Strep-Cy5 (2 hrs incubation) in the absence (left panel) or presence (right panel) of MCa_b (4 µM) in wild-type CHO cells. Scale bars: 25 µm (left) and 15 µm (right bar). (B) Cell distribution of MCa_b-Strep-Cy5 in mutant CHO cells. Scale bars: 15 µm (left) and 20 µm (right bar). Code colors: blue (Strep-Cy5), red (DHE, nuclei) and green (Concanavalin A, plasma membrane).

Fig. 6. MCa_b-Strep-Cy5 entry and endocytosis. (A) Endocytic route of entry of MCa_b-Strep-Cy5. Various CHO cell lines (wild-type, upper panels; pgsB-618, middle panels; pgsD-677, lower panels) were incubated 2 hrs with 1 µM of MCa_b-Strep-Cy5, washed and incubated with 50 nM lysotracker red DND-99 for 20 min right before confocal acquisition. Scale bars: 10 µm (upper panels) and 11 µm (middle and lower panels). (B) Different endocytic entry pathways for transferrin-Alexafluor 488 and MCa_b-Strep-Cy5. Confocal immunofluorescence images of living wild-type or mutant CHO cells to compare the cell distribution of transferrin-Alexafluor 488 and MCa_b-Strep-Cy5. Cells were incubated 2 hrs with 1 µM MCa_b-Strep-Cy5 (blue) along with 25 µg/ml transferrin-Alexafluor 488 (green), washed and immediately analyzed by confocal microscopy. Scale bars: 5 µm.

Fig. 7. Expression of the dominant-negative dynamin 2 K44A mutant blocks clathrin-mediated endocytosis and transferring entry, but spares MCa_b-Strep-Cy3 entry. (A) Transferrin entry is inhibited in dynamin 2 K44A transfected wild-type and pgsB-618 mutant CHO cells. (B) MCa_b-Strep-Cy3 entry is

preserved in dynamin 2 K44A transfected wild-type and pgsB-618 mutant CHO cells. Scale bars: 10 μM. Note that expression of dynamin 2 K44A mutant was always less in pgsB-618 mutant CHO cells than in wild-type CHO cells, possibly due to a role of GAGs in plasmid entry.

Fig. 8. Effect of endocytic inhibitors on the entry of transferrin-Alexafluor 488 and MCa_b-Strep-Cy5. Data are expressed in percentage of mean control fluorescence as assessed by FACS. Average data from three experiments. (A) Data for wild-type CHO cells. (B) Data for pgsB-618 CHO cells. Significance is provided as a deviation of three times the SD value from 100% (denoted as asterisks).

Fig. 9. Effect of MCa_b / strep ratio on the cell penetration of strep. (A) Effect of MCa_b / Strep-Cy3 ratio on the total entry of Strep-Cy3 in wild-type CHO cells. (B) Effect of an 8-fold molar excess of non-biotinylated MCa on the penetration of MCa_b-Strep-Cy3 at a 1:1 molar ratio. (C) Effect of 5 mM amiloride on Strep-Cy3 entry into wild-type CHO cells as a function of MCa_b / Strep-Cy3 ratio. Significance is provided as a deviation of three times the SD value from 100% (denoted as asterisks). Strep-Cy3 concentration was kept constant at 1 μM in all experiments.

FIGURE 1 - RAM et al.

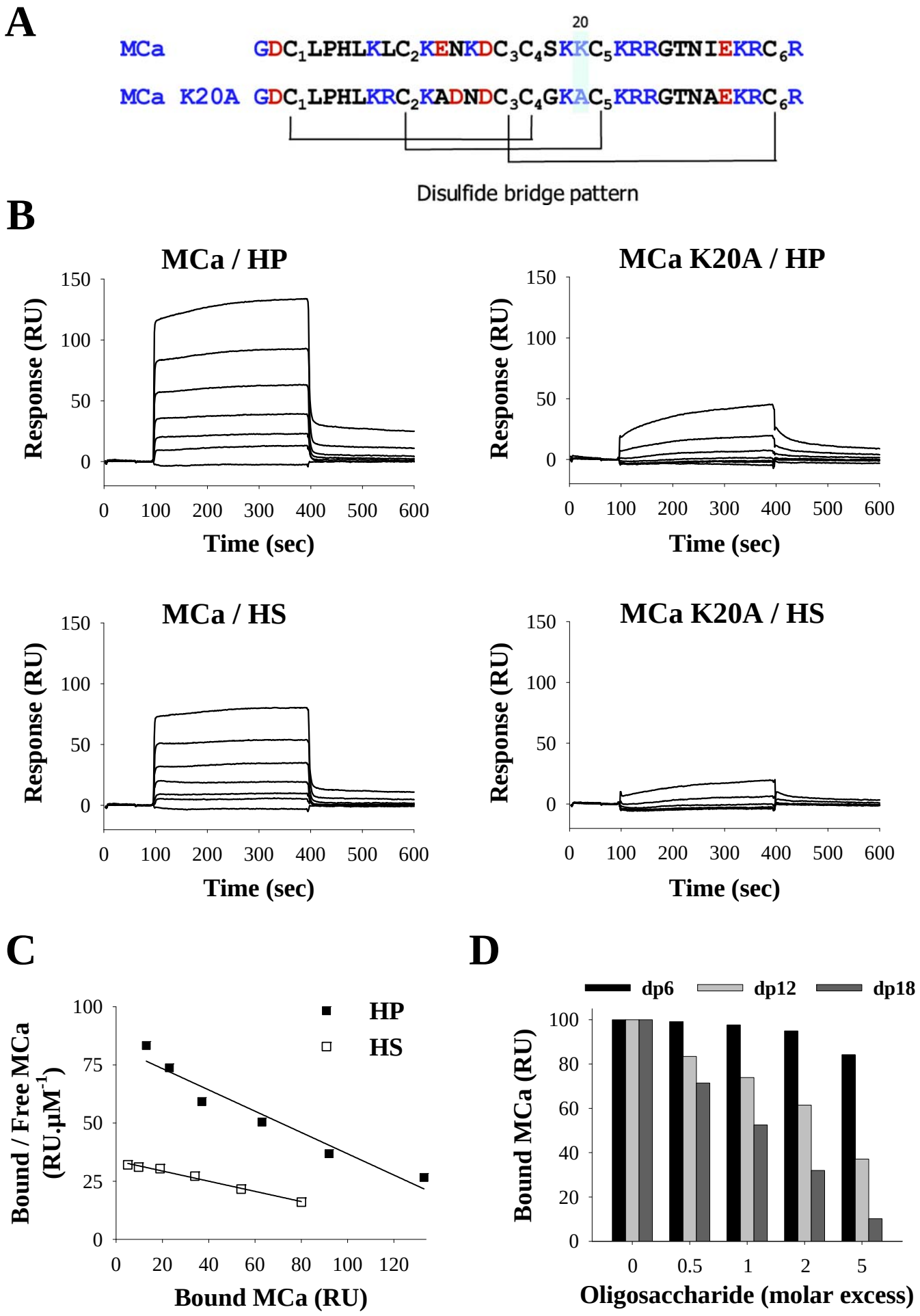

Figure 2 - RAM et al.

A

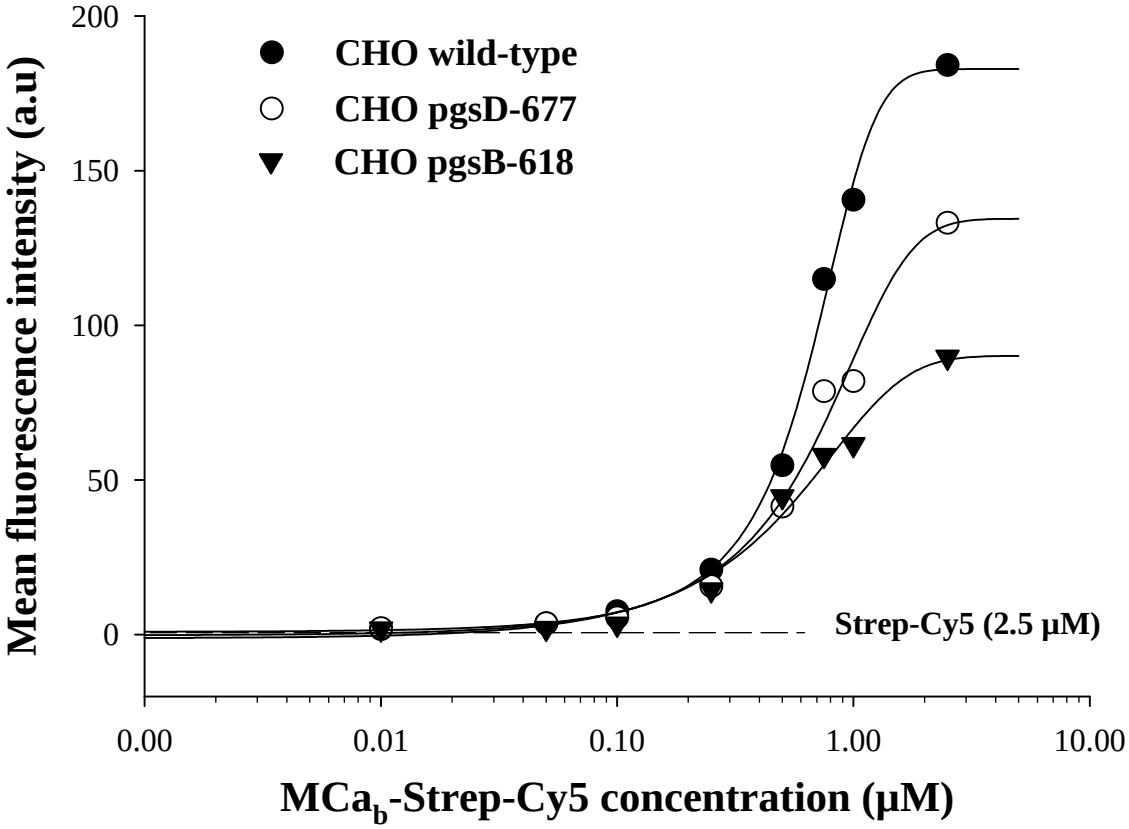

B

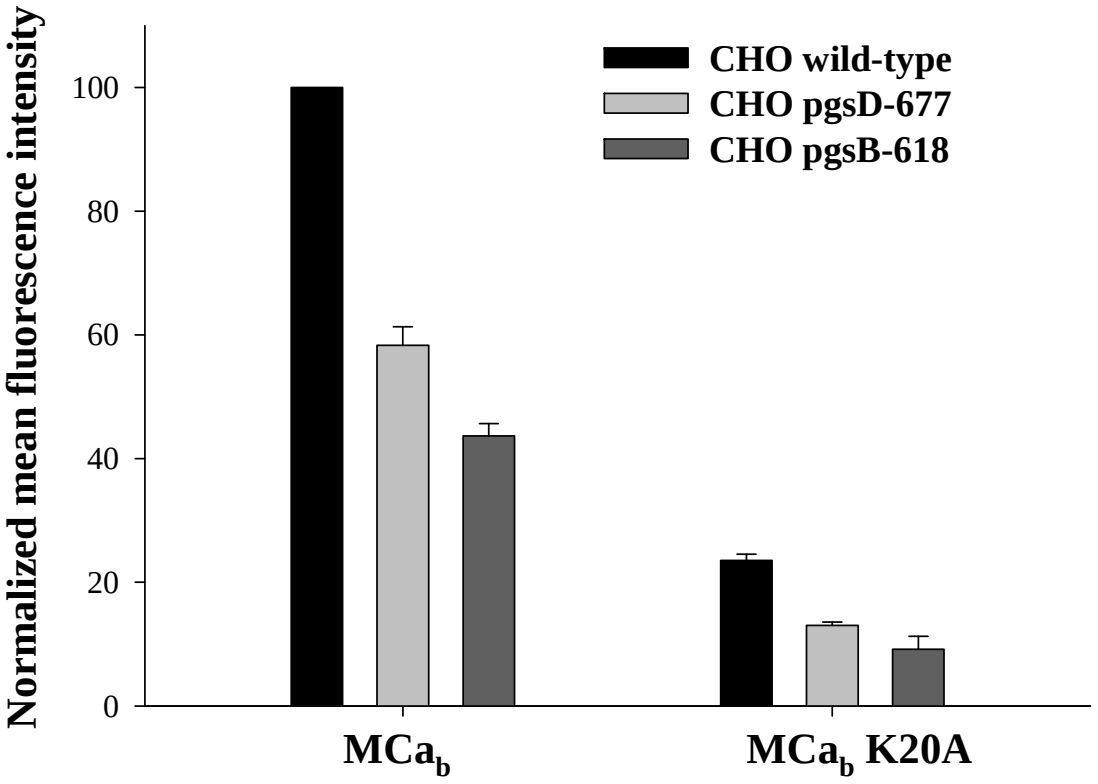

FIGURE 3 - RAM et al.

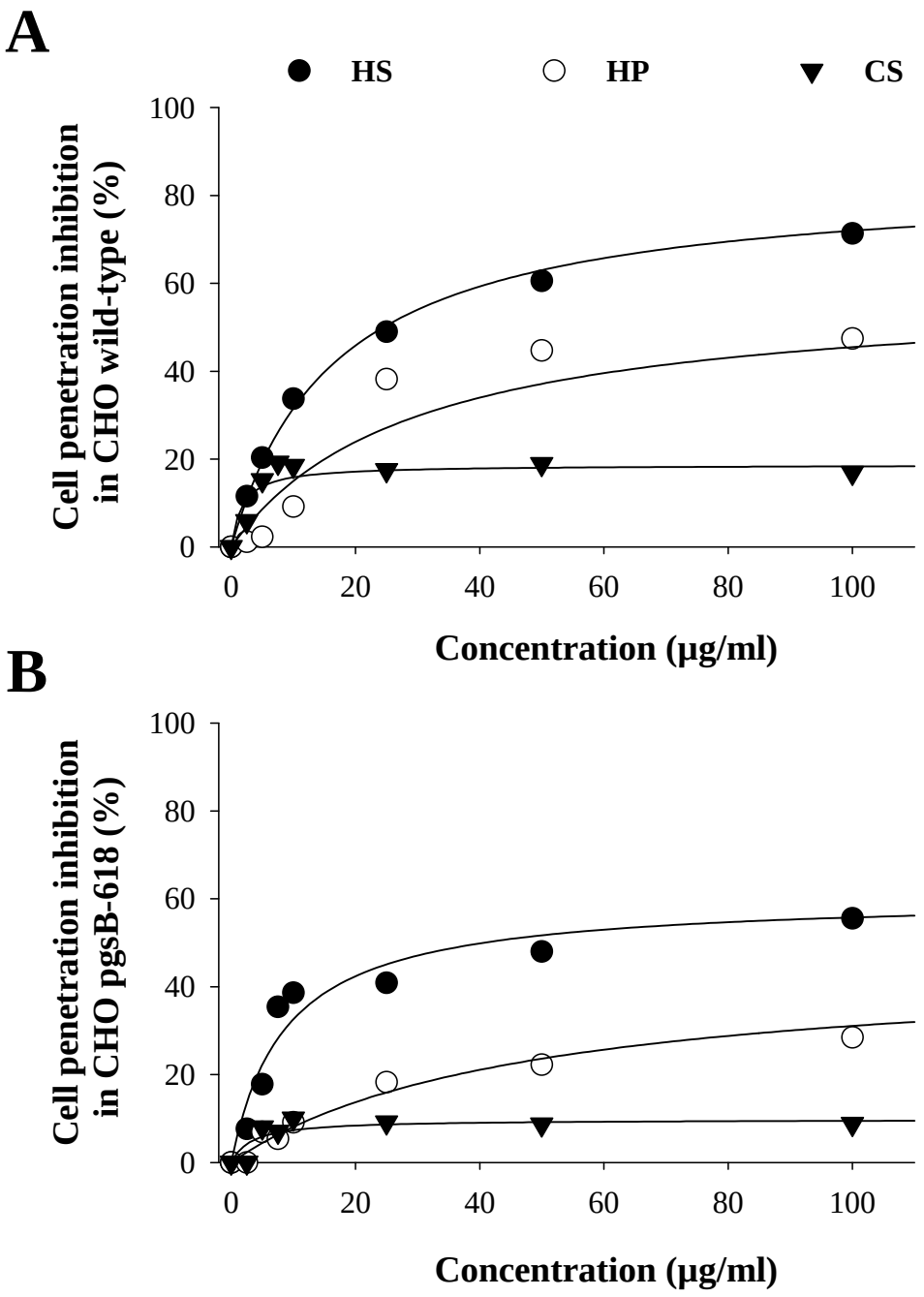

FIGURE 4 – RAM et al.

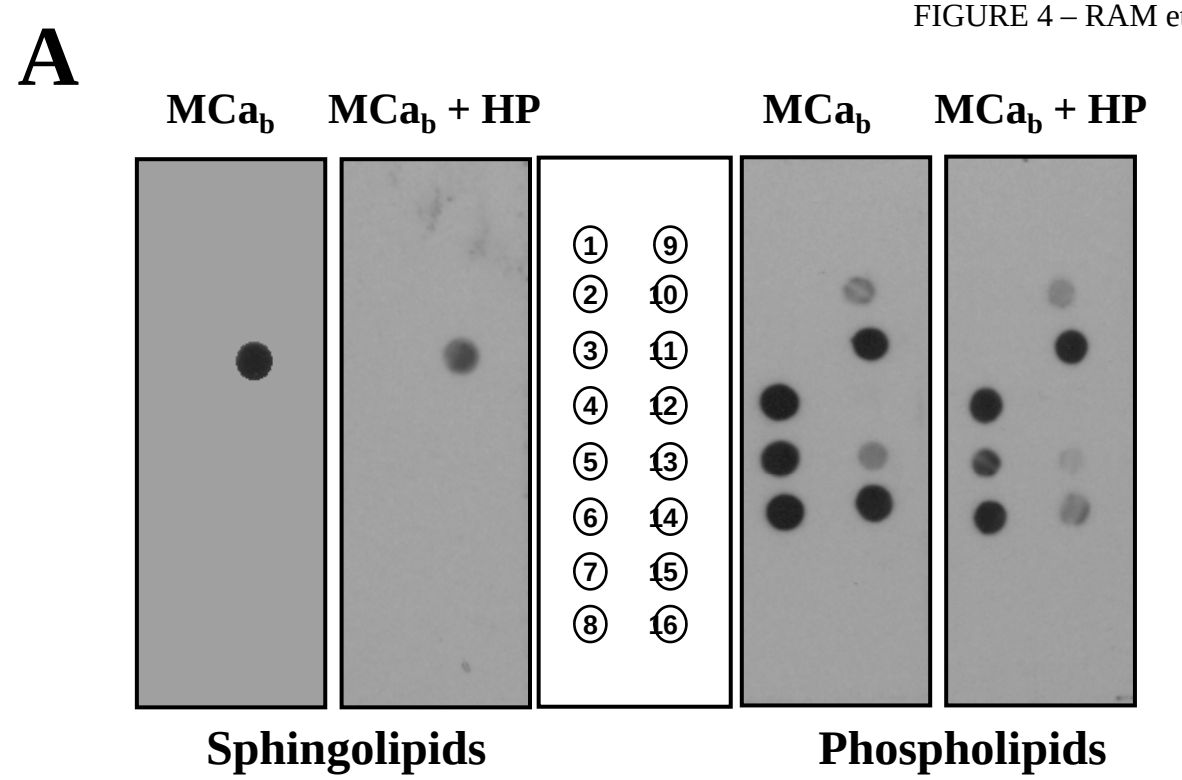

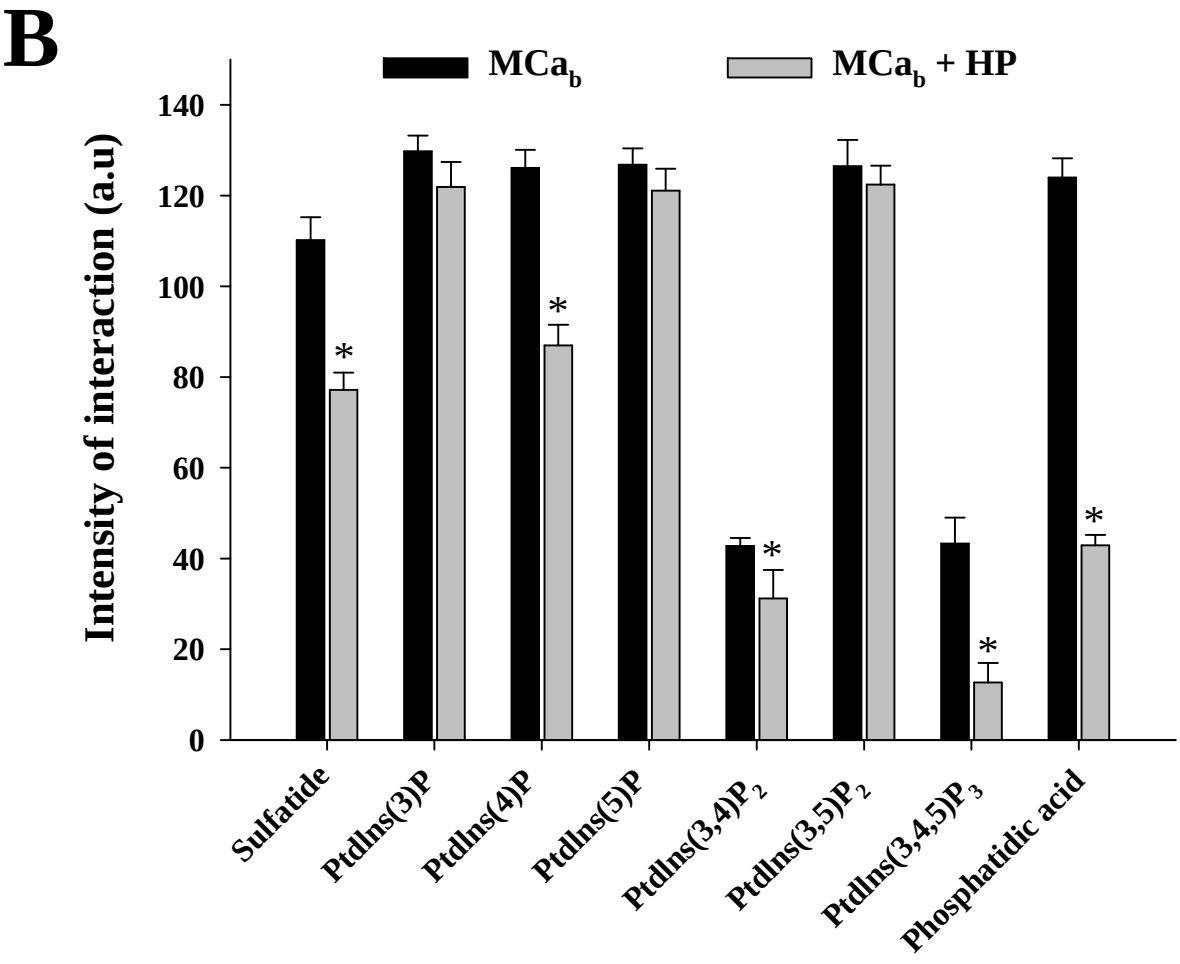

FIGURE 5 – RAM et al.

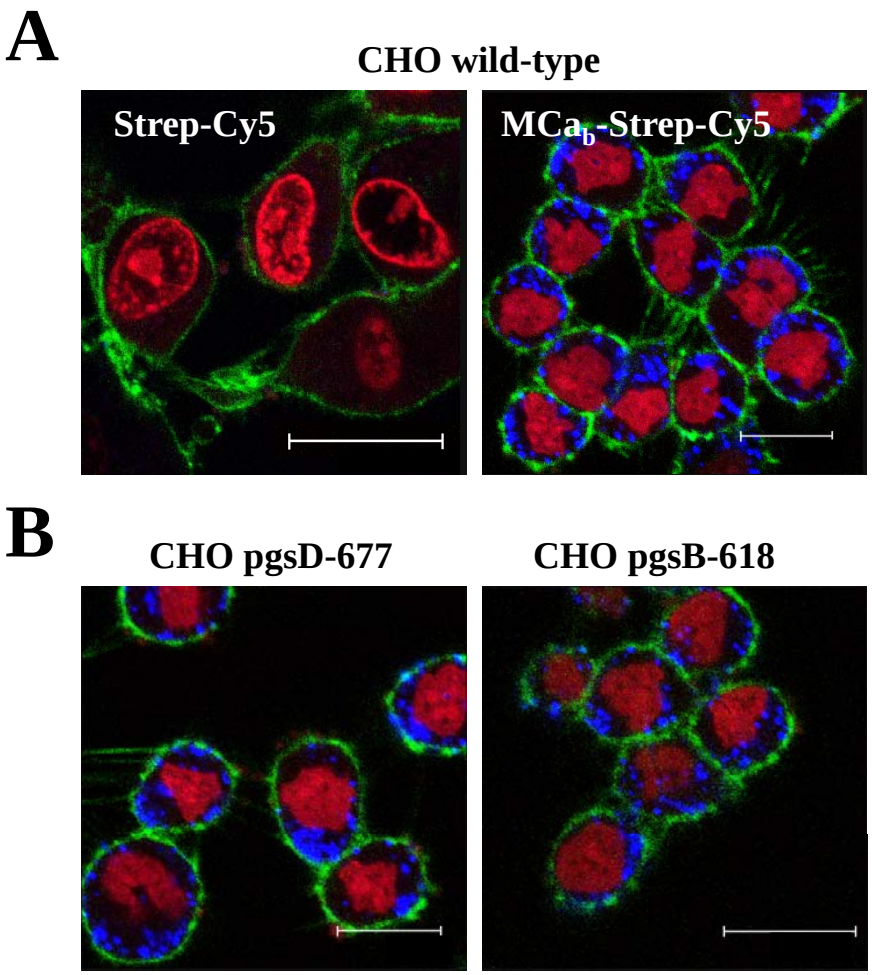

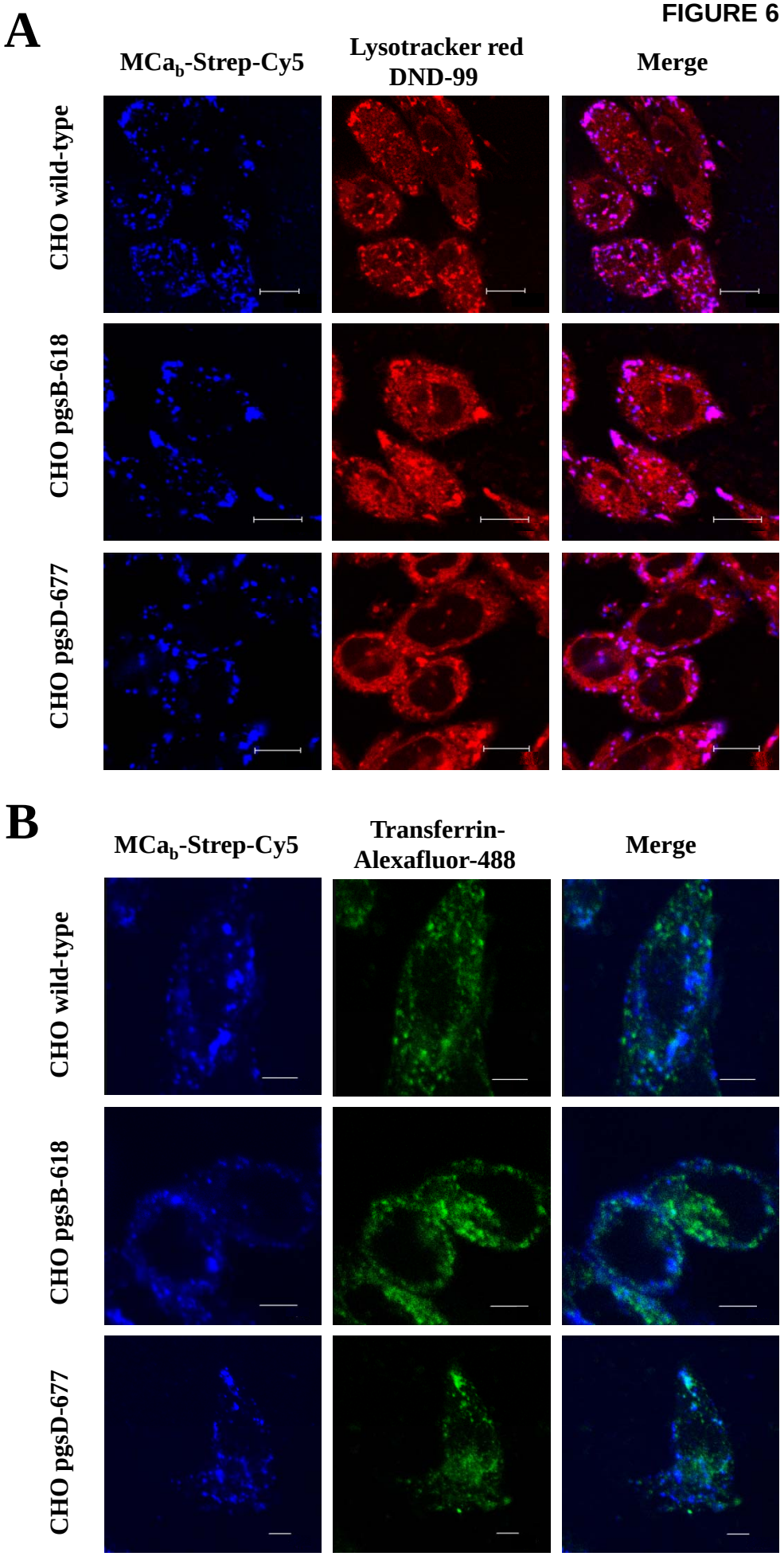
A
MCa$_b$-Strep-Cy5
Lysotracker red DND-99
Merge
CHO wild-type
CHO pgsB-618
CHO pgsD-677
B
MCa$_b$-Strep-Cy5
Transferrin-Alexafluor-488
Merge
CHO wild-type
CHO pgsB-618
CHO pgsD-677

FIGURE 7 – RAM et al.

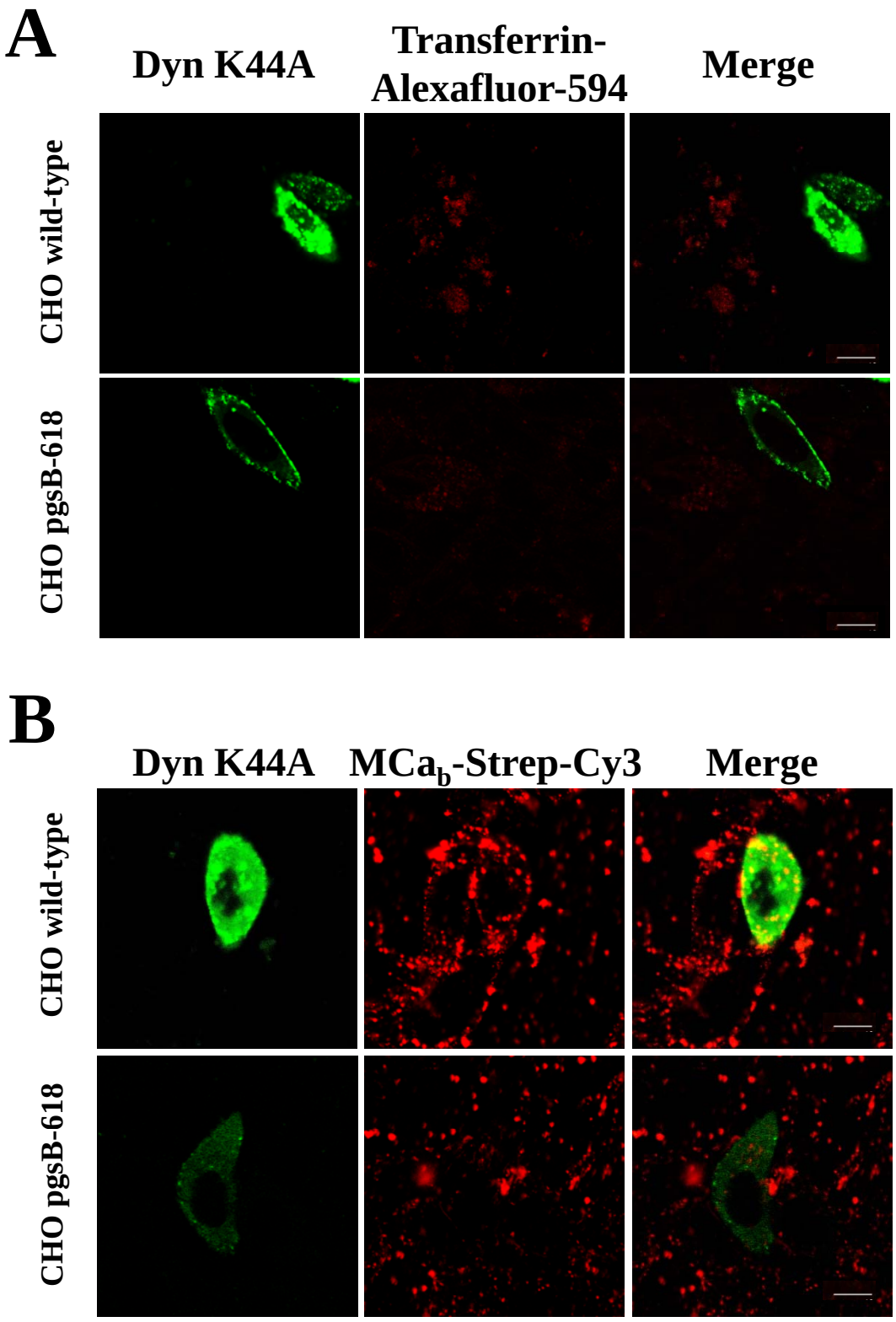

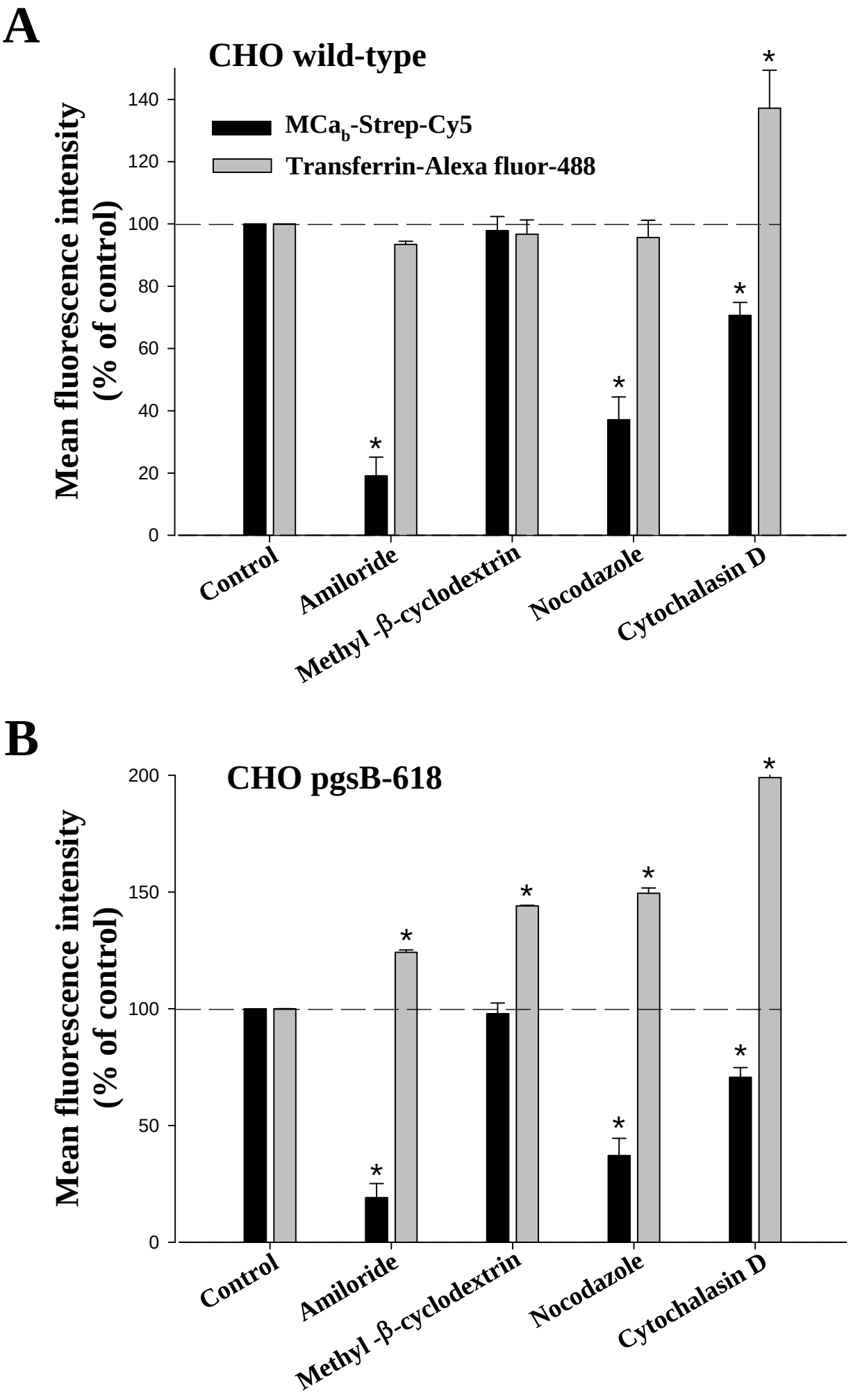
A
CHO wild-type
MCa$_b$-Strep-Cy5
Transferrin-Alexa fluor-488
Mean fluorescence intensity (% of control)
0
20
40
60
80
100
120
140
*
Control
Amiloride
Methyl -β-cyclodextrin
Nocodazole
Cytochalasin D
B
CHO pgsB-618
Mean fluorescence intensity (% of control)
0
50
100
150
200
*
Control
Amiloride
Methyl -β-cyclodextrin
Nocodazole
Cytochalasin D

FIGURE 9 - RAM et al.